Substrate Integrated Waveguide Bandpass Filter With Asymmetric Response Using Frequency-Dependent Coupling

Amit Ranjan Azad(1), Gunjan Srivastava(2), and Akhilesh Mohan(3)
(1) Department of ECE, IIIT Kalyani, West Bengal - 741235, India, amitranjanazad@iiitkalyani.ac.in
(2) Department of ECE, Graphic Era University Dehradun, Uttarakhand - 248002, India, gunjansrivastava.ece@geu.ac.in
(3) Department of ECE, IIT Roorkee, Uttarakhand - 247667, India, am@ece.iitr.ac.in

Abstract

This paper presents a substrate integrated waveguide (SIW) bandpass filter with asymmetric response. The fundamental mode of the SIW cavity resonators arranged in a triplet coupling scheme is used to create the passband. Moreover, the asymmetric frequency response is realized by employing the frequency-dependent cross-coupling which produces two transmission zeros (TZs) above the passband. The filter operates at 5.5 GHz and the fractional bandwidth (FBW) is 4%. The designed filter is fabricated and measured for experimental validation. The filter has several practical applications including WiFi networks, wireless backhaul links, and IoT devices.

1. Introduction

The accelerated advancements of wireless communication systems require planar microwave components with low loss, low cost, light weight, and easy fabrication and integration. The substrate integrated waveguide (SIW) is a promising solution to fulfill the above requirements due to owing the advantages of both planar and non-planar structures [1]. Various high performance bandpass filters have been reported using SIW technique. Moreover, the transmission zeros (TZs) are generated near the passband to improve filter selectivity. However, some applications may require bandpass filters with asymmetric frequency response where the selectivity is higher on only one side of the passband [2–17]. In order to realize asymmetric response, the mixed electric and magnetic coupling between the SIW cavity resonators is exploited [2–5]. Though the proposed filters exhibit asymmetric frequency response, it is sometimes difficult to generate the TZs at appropriate positions. The SIW bandpass filters having asymmetric response are reported using dual-mode cavity with mixed source-load coupling and coupling of higher-order modes [6, 7]. In [8, 9], the non-resonating nodes (NRNs) in SIW and coaxial SIW technology are used to design filters with asymmetric response. However, the use of higher-order modes and additional resonators as NRNs increases the overall filter size. In order to reduce the size of the bandpass filters with asymmetric response, compact hybrid structures using SIW, coplanar waveguide (CPW) and stripline resonators are discussed [10–12]. The filters demonstrate the advantages of reduced size; however, it is usually preferred to utilize similar resonators to constitute the passband because the unloaded quality factor of CPW and stripline resonators are lower than that of the SIW cavity resonator.

The filter size can also be reduced by utilizing the half-mode SIW (HMSIW), the quarter-mode SIW (QMSIW), and the eighth-mode SIW (EMSIW) cavity resonators to design miniaturized bandpass filters with asymmetric response [13, 14]. Though the filter size is reduced, but the reported compact structures have the disadvantages of leakage loss from the open sidewalls. Another approach to design SIW bandpass filters with asymmetric response is the utilization of frequency-dependent coupling between resonators either in the main path or in the cross-coupling path [15–17]. However, these filters suffer from larger footprint caused by microstrip to SIW transition and additional SIW cavity for the realization of frequency-dependent coupling.

In this paper, a third-order cross-coupled SIW bandpass filter with asymmetric frequency response is presented. The passband is produced by the dominant TE_{101} mode of the cavity. The frequency-dependent coupling is realized in the cross-coupling path. Consequently, two TZs are created above the passband and an asymmetric response is obtained with higher upper selectivity. The filter analysis and design are presented. Moreover, the simulation data of the filter is supported by the measurement results.

2. Filter Analysis and Design

A third-order bandpass filter with asymmetric response using frequency-dependent cross-coupling is designed using SIW technology. The center frequency (CF) and fractional bandwidth (FBW) of the filter are f_0 = 5.5 GHz and Δ = 4%, respectively. The filter is constructed on Rogers RO4003C substrate (ε_r = 3.55, h = 0.508 mm, and tanδ = 0.0027). The full-wave EM simulation tool Ansys HFSS is used for all simulations. The filter configuration and coupling scheme are shown in Figure 1. The filter consists of three SIW cavity resonators coupled in triplet scheme. The constant direct-coupling between resonators 1–2 and 2–3 is achieved by opening a window between

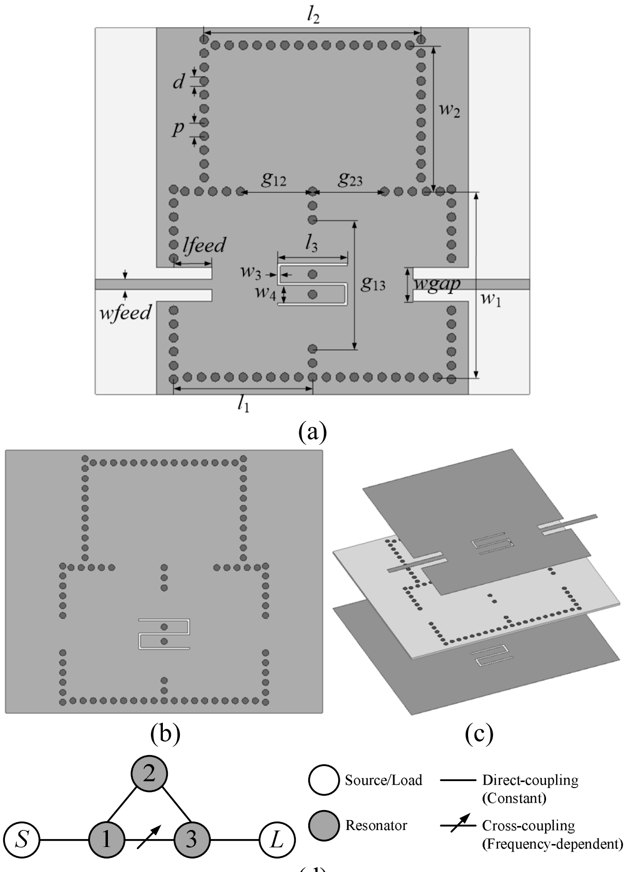

Figure 1. Filter configuration (a) Top view (b) Bottom view (c) Isometric view (d) Coupling scheme.

the cavities. Moreover, in order to enable the frequency-dependent cross-coupling between resonators 1–3, a via-less gap is formed and two meander slotlines are placed at the top and bottom metal planes, as shown in Figure 1(a)–(c). Additionally, two via-holes are inserted at the centers of the strips formed by the meander slotlines to connect the strips, as discussed and presented in [16]. The filter is synthesized based on a generalized Chebyshev response in triplet configuration with two TZs placed at normalized angular frequencies ω = 2 and ω = 3.5 and a passband return loss of 20 dB. The normalized coupling matrix of the filter is given in (1), which is extracted using the optimization-based technique reported in [18]. Figure 2 plots the synthesized response of the filter in normalized and de-normalized frequency. It can be seen that the filter has an asymmetric response with two TZs created at 5.73 and 5.91 GHz, as shown in Figure 2(b).

$$M = \begin{array}{c} \\ \boldsymbol{S} \\ \boldsymbol{1} \\ \boldsymbol{2} \\ \boldsymbol{3} \\ \boldsymbol{L} \end{array} \begin{array}{ccccc} \boldsymbol{S} & \boldsymbol{1} & \boldsymbol{2} & \boldsymbol{3} & \boldsymbol{L} \\ \end{array} \begin{bmatrix} 0 & 1.073 & 0 & 0 & 0 \\ 1.073 & 0.037 & 0.744 & 0.729-0.151\omega & 0 \\ 0 & 0.744 & -0.709 & 0.744 & 0 \\ 0 & 0.729-0.151\omega & 0.744 & 0.037 & 1.073 \\ 0 & 0 & 0 & 1.073 & 0 \end{bmatrix} \quad (1).$$

The filter design parameters based on the desired CF and bandwidth (BW) can be determined using the elements of the normalized coupling matrix. The normalized coupling matrix is de-normalized using the relations given as [19]:

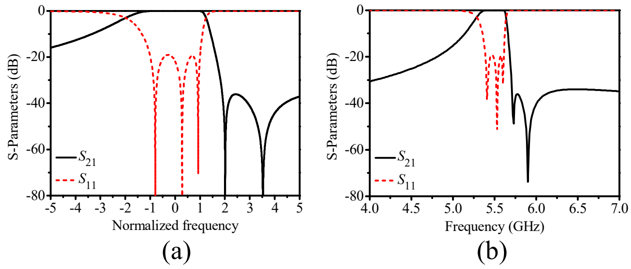

Figure 2. Synthesized response (a) Normalized frequency (b) De-normalized frequency.

$$Q_e = \frac{1}{\mathrm{FBW} \cdot M_{S1}^2}, \quad k_{ij} = \mathrm{FBW} \cdot M_{ij}, \quad \mathrm{FBW} = \frac{\mathrm{BW}}{f_0} \quad (2).$$

where Q_e is the external quality factor, k_{ij} is the coupling coefficient between resonators i and j, and f_0 is the CF of the bandpass filter. The desired external quality factor Q_e and the coupling coefficient k for given specifications are obtained as: Q_e = 21.71 and k_{12} = k_{23} = 0.0298. The self-resonant frequencies of the resonators are given as [20]: f_{01} = f_{03} = 5.496 GHz and f_{02} = 5.577 GHz. The initial dimensions of the SIW cavity with the dominant TE_{101} mode resonating at 5.5 GHz can be determined using the formulas given as [19]:

$$f_{\mathrm{TE}101} = \frac{c}{2\sqrt{\varepsilon_r}} \sqrt{\left(\frac{1}{l_e}\right)^2 + \left(\frac{1}{w_e}\right)^2} \quad (3).$$

$$l_e = l - \frac{d^2}{0.95p}, \quad w_e = w - \frac{d^2}{0.95p} \quad (4).$$

where c denotes the free-space light velocity, ε_r is the dielectric constant of the substrate, d is the metalized via-hole diameter, and p is the adjacent via-holes distance. The fixed parameter values of d = 1 mm and p = 1.6 mm are used in this study. A SIW cavity resonator fed with a 50 Ω microstrip line is simulated to determine Q_e. The Q_e of a resonator can be calculated as [20]:

$$Q_e = \frac{f_0}{\Delta f_{\pm 90^\circ}} \quad (5).$$

where f_0 is the resonant frequency of the resonator and $\Delta f_{\pm 90^\circ}$ is the relative bandwidth obtained by the phase change of ±90° with respect to the absolute phase at f_0. The Q_e variation with change in *lfeed* is plotted in Figure 3. It can be seen that the Q_e decreases as *lfeed* is increased from 1 to 5 mm. Two coupled SIW cavity resonators with weak I/O coupling is simulated to find k. The k between two resonators is determined as [20]:

$$k = \frac{f_1^2 - f_2^2}{f_1^2 + f_2^2} \quad (6).$$

where f_1 and f_2 are the high and low resonant frequencies, respectively. The direct-coupling coefficient k_{12} (or k_{23}) against the varied window size g_{12} (or g_{23}) are extracted and plotted in Figure 4. It is found that the k_{12} increases as

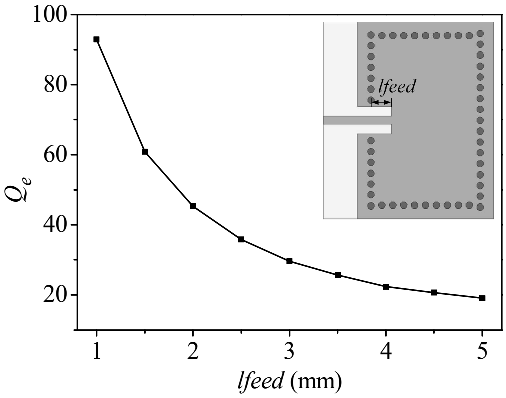

Figure 3. Q_e variation against *lfeed*.

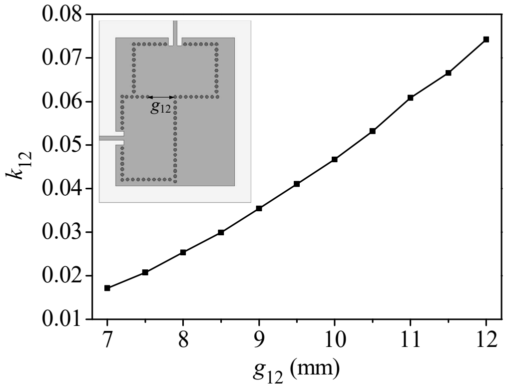

Figure 4. k_{12} variation against g_{12}.

g_{12} increases from 7 to 12 mm. To synthesize the proper frequency-dependent coupling, the magnitude and phase of S_{21} must be similar to those resulting from the coupling matrix M. The frequency response of the cross-coupled resonators 1–3 can be found by the coupling matrix M_{13} given in (7), which is obtained by removing the first, third and fifth rows and columns of the coupling matrix M.

$$M_{13} = \begin{bmatrix} 0.037 & 0.729 - 0.151\omega \\ 0.729 - 0.151\omega & 0.037 \end{bmatrix} \quad (7).$$

Figure 5(a) illustrates the coupling structure to realize the frequency-dependent cross-coupling between resonators 1–3. The dimensions of the frequency-dependent coupling structure are: $l_1 = 16$, $w_1 = 21.3$, $l_3 = 8.4$, $w_3 = 0.2$, $w_4 = 2$, $g_{13} = 16.9$, $wfeed = 1.2$, $lfeed = 1$, and $wgap = 4$ (all in mm). The magnitude and phase of S_{21} obtained from the coupling matrix M_{13} and those obtained from simulation are plotted in Figure 5(b). Note that the synthesized and simulated responses are obtained under weak I/O coupling ($M_{S1} = M_{3L} = 0.5$) to realize exact coupling coefficient and the position of the TZ. It can be found that the magnitude and phase of the synthesized and simulated S_{21} show a good match which illustrates that the desired frequency-dependent coupling is realized.

3. Measurement Results

The bandpass filter is designed for given specifications using the results presented above, as shown in Figure 1. The optimized filter dimensions (in mm) are: $l_1 = 16$, $l_2 = 25$, $w_1 = 21.5$, $w_2 = 16.95$, $l_3 = 8$, $w_3 = 0.2$, $w_4 = 2$, $g_{12} = g_{23} = 8.3$, $g_{13} = 15$, $wfeed = 1.2$, $lfeed = 4.45$, and $wgap = 4$. The simulation results show that the CF of the filter is $f_0 = 5.5$ GHz and the 1-dB FBW is $\Delta = 4.67\%$. The mid-band insertion loss is 1.67 dB, and the passband return loss is larger than 16 dB. Moreover, two TZs are created at $TZ_1 = 5.78$ GHz and $TZ_2 = 6.01$ GHz, and as a result, an asymmetric frequency response is produced.

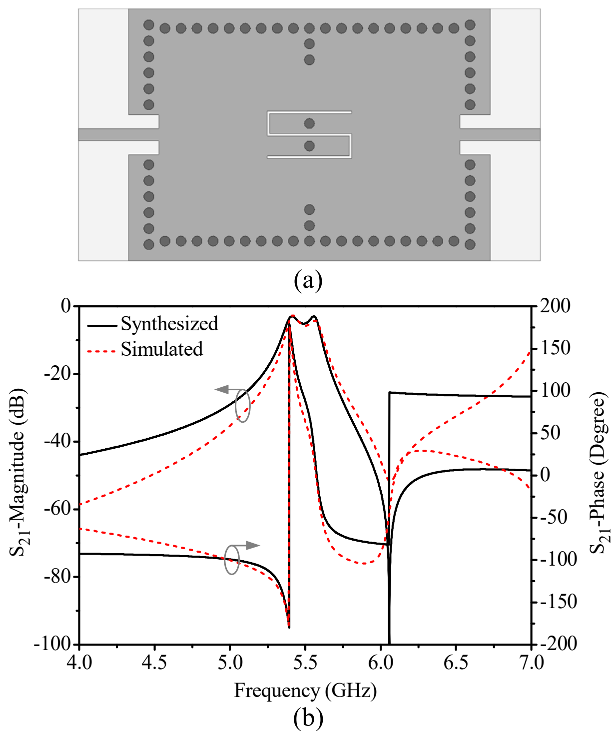

Figure 5. (a) Coupling structure to realize frequency-dependent cross-coupling (b) S_{21} magnitude and phase of synthesized and simulated response.

To validate the simulation results, the filter is constructed and measured. The fabricated filter photograph is depicted in Figure 6(a), and Figure 6(b) presents the synthesis, simulation, and measurement data. The measured results show that the filter is centered at $f_0 = 5.52$ GHz with a 1-dB FBW of $\Delta = 4.17\%$. The minimum in-band insertion loss is around 2.5 dB, and the return loss in the passband is greater than 12 dB. The filter exhibits sharp upper selectivity due to the two TZs located at 5.84 and 6.03 GHz. Figure 7 plots the simulated *E*-field in the filter at 5.5 GHz (f_0), 5.78 GHz (TZ_1), and 6.01 GHz (TZ_2). It can be observed that the passband is created at f_0 while the transmission is blocked at TZ_1 and TZ_2 resulting in an asymmetric response. Moreover, the synthesis, simulation and measurement results show an admissible agreement among them. However, some discrepancies are seen in the measured results because of the fabrication tolerances and connector losses. The comparison of the presented filter with the reported SIW bandpass filters using frequency-dependent coupling is listed in Table I. It can be noticed that the filter demonstrates the advantages of compact size, simple geometry, and favorable frequency response making it a promising component for modern wireless applications.

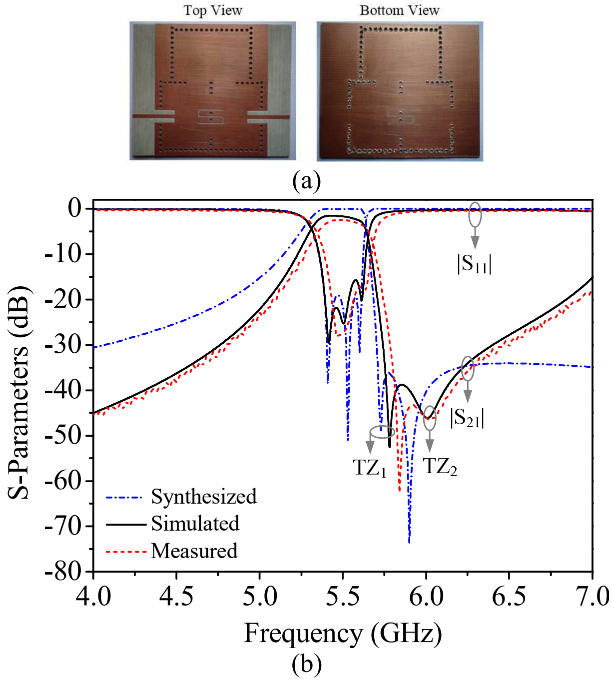

Figure 6. (a) Fabricated filter photograph (b) Synthesized, simulated and measured results.

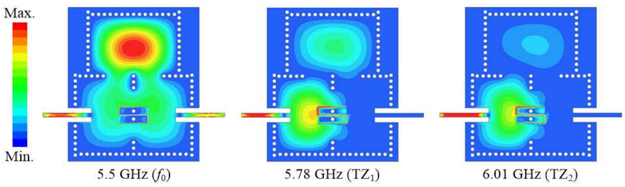

Figure 7. Simulated *E*-field in the filter at 5.5 GHz (f_0), 5.78 GHz (TZ$_1$), and 6.01 GHz (TZ$_2$).

TABLE I

COMPARISON WITH REPORTED SIW BANDPASS FILTERS USING FREQUENCY-DEPENDENT COUPLING

Ref.	f_0 (GHz)	Order	IL (dB)	FBW (%)	TZs	Size ($\lambda_g \times \lambda_g$)
[15]	5.25	4	2.4	5.7	2	2.09×2.03*
[16]	4.85	3	3	3.71	2	2.62×1.37*
[17]	5.02	5	1.64	3	2	3.38×1.47*
This Work	**5.52**	**3**	**2.5**	**4.17**	**2**	**1.11×1.33**

IL: Insertion Loss; FBW: Fractional Bandwidth; TZs: Transmission Zeros; *: Estimated Data.

4. Conclusion

A third-order SIW filter with asymmetric response using frequency-dependent cross-coupling was presented in this paper. The desired frequency-dependent cross-coupling is realized by appropriately matching the magnitude and phase characteristics of simulation and synthesis data. The close agreement among the synthesis, simulation, and measurement responses demonstrate the validity of the approach. The presented filter shows the advantages of simple structural configuration and asymmetric frequency response with improved upper selectivity. The filter can be used for WiFi applications, wireless backhaul links, unmanned aerial vehicles, and IoT devices and networks.

5. References

[1] D. Deslandes, K. Wu, "Integrated microstrip and rectangular waveguide in planar form," *IEEE Microwave and Wireless Components Letters*, **11**, 2, Feb. 2001, pp. 68–70.

[2] B. Potelon *et al.*, "Design of a substrate integrated waveguide (SIW) filter using a novel topology of coupling," *IEEE Microwave and Wireless Components Letters*, **18**, 9, Sep. 2008, pp. 596–598.

[3] W. Shen *et al.*, "Novel substrate integrated waveguide filters with mixed cross coupling (MCC)," *IEEE Microwave and Wireless Components Letters*, **19**, 11, Nov. 2009, pp. 701–703.

[4] A. R. Azad, D. K. Jhariya, and A. Mohan, "Substrate-integrated waveguide cross-coupled filters with mixed electric and magnetic coupling structure," *International Journal of Microwave and Wireless Technologies*, **10**, 8, Oct. 2018, pp. 896–903.

[5] P. Chu *et al.*, "Substrate integrated waveguide filter with flexible mixed coupling," *IEEE Transactions on Microwave Theory and Techniques*, **71**, 9, Sep. 2023, pp. 4003–4011.

[6] Z. Xu, Y. Shi, C. Xu, and P. Wang, "A novel dual mode substrate integrated waveguide filter with mixed source-load coupling (MSLC)," *Progress In Electromagnetics Research*, **136**, Jan. 2013, pp. 595–606.

[7] X.-P. Chen and K. Wu, "Self-packaged millimeter-wave substrate integrated waveguide filter with asymmetric frequency response," *IEEE Transactions on Components, Packaging and Manufacturing Technology*, **2**, 5, May 2012, pp. 775–782.

[8] R. Li and G. Du, "A SIW filter with asymmetric frequency response by non-resonating node," *Journal of Electromagnetic Waves and Applications*, **27**, 12, Jul. 2013, pp. 1550–1556.

[9] S. Sirci *et al.*, "Advanced filtering solutions in coaxial SIW technology based on singlets, cascaded singlets, and doublets," *IEEE Access*, **7**, Mar. 2019, pp. 29901–29915.

[10] P. Chu *et al.*, "A planar bandpass filter implemented with a hybrid structure of substrate integrated waveguide and coplanar waveguide," *IEEE Transactions on Microwave Theory and Techniques*, **62**, 2, Feb. 2014, pp. 266–274.

[11] M. R. Jiao, F. Zhu, P. Chu, W. Yu, and G. Q. Luo, "Compact hybrid bandpass filters using substrate-integrated waveguide and stripline resonators," *IEEE Transactions on Microwave Theory and Techniques*, **72**, 1, Jan. 2024, pp. 391–400.

[12] Y. Zheng and Y. Dong, "Miniaturized hybrid filter using stripline and *LC*-loaded SIW resonators," *IEEE Transactions on Circuits and Systems–II: Express Briefs*, **69**, 9, Sep. 2022, pp. 3719–3723.

[13] D. Liu and Y. Dong, "Compact low-loss half-mode substrate integrated waveguide filter with controllable transmission zeros," *IEEE Transactions on Circuits and Systems–II: Express Briefs*, **69**, 11, Nov. 2022, pp. 4248–4252.

[14] P. Kim and Y. Jeong, ''Compact and wide stopband substrate integrated waveguide bandpass filter using mixed quarter- and one-eighth modes cavities,'' *IEEE Microwave and Wireless Components Letters*, **30**, 1, Jan. 2020, pp. 16–19.

[15] L. Szydlowski *et al.*, "A substrate integrated waveguide (SIW) bandpass filter in a box configuration with frequency-dependent coupling," *IEEE Microwave and Wireless Components Letters*, **22**, 11, Nov. 2012, pp. 556–558.

[16] L. Szydlowski *et al.*, "A trisection filter design with negative slope of frequency-dependent crosscoupling implemented in substrate integrated waveguide (SIW)," *IEEE Microwave and Wireless Components Letters*, **23**, 9, Sep. 2013, pp. 456–458.

[17] G. Macchiarella *et al.*, "Design of inline waveguide filters with frequency-variant couplings producing transmission zeros," *IEEE Transactions on Microwave Theory and Techniques*, **69**, 8, Aug. 2021, pp. 3746–3758.

[18] A. R. Azad and A. Mohan, "Synthesis of cross-coupled resonator filters with frequency-dependent coupling using comprehensive learning particle swarm optimization," in *Proc. IEEE MTT-S International Microwave and RF Conference (IMaRC)*, Kolkata, India, Nov. 2018, pp. 1–4.

[19] X.-P. Chen, K. Wu, "Substrate integrated waveguide cross-coupled filter with negative coupling structure," *IEEE Transactions on Microwave Theory and Techniques*, **56**, 1, Jan. 2008, pp. 142–149.

[20] J.-S. Hong, M. J. Lancaster, *Microstrip Filters for RF/Microwave Applications*. New York: John Wiley & Sons, 2001, pp. 235–272.